Wetlands (2016) 36:201–213
DOI 10.1007/s13157-015-0730-7

ORIGINAL RESEARCH

A Framework to Combine Three Remotely Sensed Data Sources for Vegetation Mapping in the Central Florida Everglades

Caiyun Zhang[1] · **Donna Selch**[1] · **Hannah Cooper**[1]

Received: 29 September 2015 / Accepted: 21 December 2015 / Published online: 29 December 2015

Abstract A framework was designed to integrate three complimentary remotely sensed data sources (aerial photography, hyperspectral imagery, and LiDAR) for mapping vegetation in the Florida Everglades. An object-based pixel/feature-level fusion scheme was developed to combine the three data sources, and a decision-level fusion strategy was applied to produce the final vegetation map by ensemble analysis of three classifiers *k*-Nearest Neighbor (*k*-NN), Support Vector Machine (SVM), and Random Forest (RF). The framework was tested to map 11 land-use/land-cover level vegetation types in a portion of the central Florida Everglades. An informative and accurate vegetation map was produced with an overall accuracy of 91.1 % and Kappa value of 0.89. A combination of the three data sources achieved the best result compared with applying aerial photography alone, or a synergy of two data sources. Ensemble analysis of three classifiers not only increased the classification accuracy, but also generated a complementary uncertainty map for the final classified vegetation map. This uncertainty map was able to identify regions with a high robust classification, as well as areas where classification errors were most likely to occur.

Keywords Data fusion · Ensemble analysis · Uncertainty analysis · Wetland land-use/land-cover level vegetation mapping

✉ Caiyun Zhang
czhang3@fau.edu

[1] Department of Geosciences, Florida Atlantic University, 777 Glades Road, Boca Raton, FL 33431, USA

Introduction

Significance of Vegetation Mapping in the Florida Everglades

The Florida Everglades is the largest subtropical wetland in the USA. It has a unique ecosystem that supports many threatened and endangered species. In the past century, human activities severely modified this imperiled ecosystem, resulting in many environmental issues in South Florida (e.g., McPherson and Halley 1996). In 2000 the U.S. Congress authorized the Comprehensive Everglades Restoration Plan (CERP) to restore the Everglades ecosystem (CERP 2015). CERP is expected to take 30 or more years to complete. Many on-going and completed projects in CERP require accurate and informative vegetation maps because restoration will cause dramatic modification to plant communities (Doren et al. 1999). The effects and progress of restoration can be measured by monitoring changes in vegetation communities (Jones 2011). Therefore, vegetation maps derived from remotely sensed data serve as valuable tools for assessing CERP restoration efforts.

Efforts of Automated Vegetation Mapping in the Florida Everglades

Vegetation maps in support of CERP are mainly from manual interpretation of large-scale aerial photographs using analytical stereo plotters (Rutchey et al. 2008). This procedure is time-consuming and labor-intensive. To address this issue, several efforts have been made to automate vegetation mapping through digital image analysis. Such efforts can be grouped into three categories. The first is the application of single-source remotely sensed data such as multispectral imagery (Rutchey and Vilchek 1994, 1999; Jensen et al. 1995;

Szantoi et al. 2015) and hyperspectral imagery (Hirano et al. 2003; Zhang and Xie 2012, 2013). Studies have shown that most available remotely sensed imagery (e.g., Landsat) could not generate classifications with reasonable accuracies in the Everglades due to limitations of spatial or spectral resolution. High spatial resolution (i.e., 5 meters or smaller) hyperspectral imagery is powerful in vegetation characterization over this region (Zhang and Xie 2012, 2013), but data collection is costly. The second is the employment of a combination of single-source remotely sensed imagery with ancillary data such as environmental variables, hydrological variables, and soil data (Griffin et al. 2011; Szantoi et al. 2013). The third is the application of multi-source remotely sensed data through data fusion techniques (Zhang et al. 2013; Zhang and Xie 2014; Zhang 2014), which integrate data and information from multiple sources to achieve refined/improved information for decision making (Gómez-Chova et al. 2015). With the increasing availability of multi-sensor, multi-temporal, and multi-resolution images, data fusion has become a valuable tool for updating wetland inventory (Kloiber et al. 2015).

Potential of Fusing Three Remotely Sensed Data Sources for Vegetation Mapping

For this study we combined three data sources for vegetation mapping including 1-m fine spatial resolution aerial photography, 30-m Earth Observing-1 (EO-1)/Hyperion hyperspectral imagery, and Light Detection And Ranging (LiDAR) data. High spatial resolution aerial photos can provide important spatial information such as texture for vegetation discrimination, but application of 1-m aerial photography alone could not produce requisite accuracy in the Everglades (Zhang and Xie 2014). Application of very high aerial imagery (20–30 centimeters) can achieve good results (Szantoi et al. 2013, 2015), but this type of data is scarce in the Everglades. Hyperspectral sensors are more powerful than traditional multispectral sensors in vegetation mapping due to their rich radiometric content (Thenkabail et al. 2011). The application of hyperspectral data has become an important area of research for wetland mapping (Adam et al. 2010). However, most of the available hyperspectral sensors such as the in-orbit spaceborne EO-1/Hyperion collect data with a relatively coarse spatial resolution (i.e., 30 meters or lower). This limits their application in the Everglades because vegetation has a high spatial and spectral heterogeneity where small patches or linear/narrow shaped vegetation covers cannot be clearly defined. LiDAR contains useful information for vegetation characterization (Lewis and Hancock 2007) and high-posting-density (i.e., >4 pts/m^2) LiDAR has been frequently combined with optical imagery to improve vegetation classification (e.g., Onojeghuo and Blackburn 2011; Zhang and Qiu 2012). However, little work has been conducted to include low-posting-density (i.e., <2 pts/m^2) LiDAR in the classification (Ke et al. 2010), especially for wetland mapping (Zhang et al. 2013; Zhang 2014). Low-posting-density LiDAR may improve vegetation classification in the unique Everglades environment.

In general, aerial photography, hyperspectral imagery, and LiDAR data have their pros and cons. High spatial resolution aerial photography is able to provide valuable spatial information and delineate a target boundary, but it cannot effectively discriminate the target due to coarse spectral resolution (Shaw and Burke 2003). Hyperspectral systems with a medium spatial resolution, such as EO-1/Hyperion, are powerful at identifying objects, but are not configured to map heterogeneous landscapes such as in the Everglades. LiDAR can complement spectral information by providing useful elevation information to improve vegetation identification (Zhang et al. 2013). A potential drawback worth mentioning is that the successful inclusion of low-posting-density LiDAR in the classification largely depends on the methods for extracting LiDAR features. Overall, these three remote sensing systems carry complimentary information, and the synergy between them has potential to automate vegetation mapping in the Everglades.

Objectives

The main objective of this study is to explore the potential of fusing aerial photography, hyperspectral imagery, and LiDAR for vegetation mapping in the Florida Everglades. To effectively fuse three data sources, object-based image analysis (OBIA), machine learning and ensemble analysis techniques were applied. Traditional pixel-based methods may lead to the "salt-and-pepper" effect in mapping heterogeneous landscapes. This issue can be overcome by OBIA techniques which first decompose an image scene into relatively homogeneous object areas and then classify these object areas instead of pixels (Blaschke 2010). Three machine learning classifiers *k*-Nearest Neighbor (*k*-NN), Support Vector Machine (SVM), and Random Forest (RF) have proven useful in classifying hyperspectral imagery and combined multi-source datasets (e.g., Chan and Paelinckx 2008; Waske et al. 2009; Mountrakis et al. 2010; Kloiber et al. 2015). In this study their performance was evaluated for classifying the fused dataset from three data sources. Recent studies have illustrated that an ensemble analysis of multiple classifiers may improve the classification or generate a more robust result (Zhang 2014, 2015). In addition, ensemble analysis can provide an uncertainty map to complement the traditional accuracy assessment techniques in remote sensing (Zhang 2014). To further understand the uncertainty analysis from multiple classifiers, ensemble analysis was also explored. The specific objectives of this study are 1) to design a framework to combine three types of remotely sensed datasets for complex wetland

mapping; and 2) to examine the benefits of ensemble analysis of multiple classifiers, as well as the potential of the uncertainty map from ensemble analysis in accuracy assessment.

Study Area and Data

Study Area

The study site is a portion of Caloosahatchee River watershed in the central Florida Everglades (Fig. 1). The Everglades occupies most of the southern peninsula of Florida and extends southward from Lake Okeechobee into the Gulf of Mexico. Lake Okeechobee serves as the "water heart" for the Everglades, and the Caloosahatchee River functions as a primary canal that conveys basin runoff and regulatory releases from Lake Okeechobee. The hydrology of this region has been severely changed because many canals were constructed along the banks of the river to support the agricultural communities associated with the river. "Get the water right" in the Caloosahatchee watershed is a key component in CERP. Response of the plant community in this region is a crucial indicator of the restoration success and detailed vegetation maps can guide the path of restoration. The selected site covers an area of about 30 km^2 presenting a total of eleven land-use/land-cover level vegetation communities which are described in Table 1.

Data

Data sources include digital aerial photography, EO-1/Hyperion hyperspectral imagery, LiDAR, and reference data. Fine spatial resolution aerial photographs were collected in November 2004 by the National Aerial Photography Program (NAPP). The U. S. Geological Survey (USGS) orthorectified these aerial photos into data products known as Digital Orthophoto Quarter Quads (DOQQs). The accuracy and quality of DOQQs meet National Map Accuracy Standards (NMAS). DOQQs with four spectral channels (Red, Green, Blue, and NIR) in a spatial resolution of 1 meter were used in this study. A color infrared composite of DOQQs for the study site is shown in Fig. 1.

Hyperspectral imagery was collected in October 2005 by the Hyperion Imaging Spectrometer onboard the EO-1 spacecraft. EO-1/Hyperion is the first spaceborne hyperspectral sensor acquiring imagery in 242 contiguous spectral bands (0.4–2.5 μm) with a spatial resolution of 30 meters. The mission of EO-1/Hyperion is to evaluate on-orbit issues for imaging spectroscopy and to assess the capabilities of a spaceborne imaging spectrometer for Earth science and observation (Folkman et al. 2001). USGS has conducted the radiometric and systematic geometric corrections for the raw scenes. The preprocessed data are delivered to users as the Level 1 Gst products.

LiDAR data were collected using Leica ALS-50 system in December 2007 to support the Florida Division of Emergency Management. The Leica ALS-50 LiDAR system collects small footprint multiple returns, and intensity at 1060 nm wavelength. The average point density for the study area is 1.2 pts/m^2. The original LiDAR point cloud data were processed by the vendor to generate the Digital Terrain Model (DTM) using Merrick Advanced Remote Sensing processing software. All the LiDAR point cloud data and DTM are available to the public at the International Hurricane Research Center website. Aerial photographs, hyperspectral data, and LiDAR were collected during the dry season (from November to April) and within a reasonable time span, which provides a good basis for evaluating vegetation mapping using data fusion techniques.

The South Florida Water Management District (SFWMD) (one partner in CERP) provided a digital vegetation map for this study. This vegetation map was built by the manual photointerpretation of 2004–2005 NAPP aerial photographs. The modified Florida Land Use, Land Cover Classification System was used in the interpretation. Features were stereoscopically interpreted using a stereo plotter and calibrated from field surveys. The reference data was compiled on screen over DOQQs, the same digital aerial photographs as those used in this study. The positional accuracy of the data meets the NMAS.

We randomly selected 738 image objects as the reference data for the study area. The number of reference objects for each class is listed in Table 1. The image objects were produced by segmenting the 1-m aerial photography, which are detailed in next section. We followed a spatially stratified data sampling strategy, in which a fixed percentage of samples were selected for each class. The number of reference objects for each class was estimated based on the image segmentation results and the digital vegetation map. The selected reference objects were manually labeled and refined by jointly checking the digital vegetation map, aerial photography, and hyperspectral imagery. The selected reference objects for each class were split into two halves with one for calibration and the other for validation. Non-vegetation objects were masked out using the digital vegetation map since the main concern of this study was vegetation.

Methodology

Data Preprocessing

Low-signal-noise ratio bands, uncalibrated bands, and severe stripping bands of the EO-1/Hyperion imagery

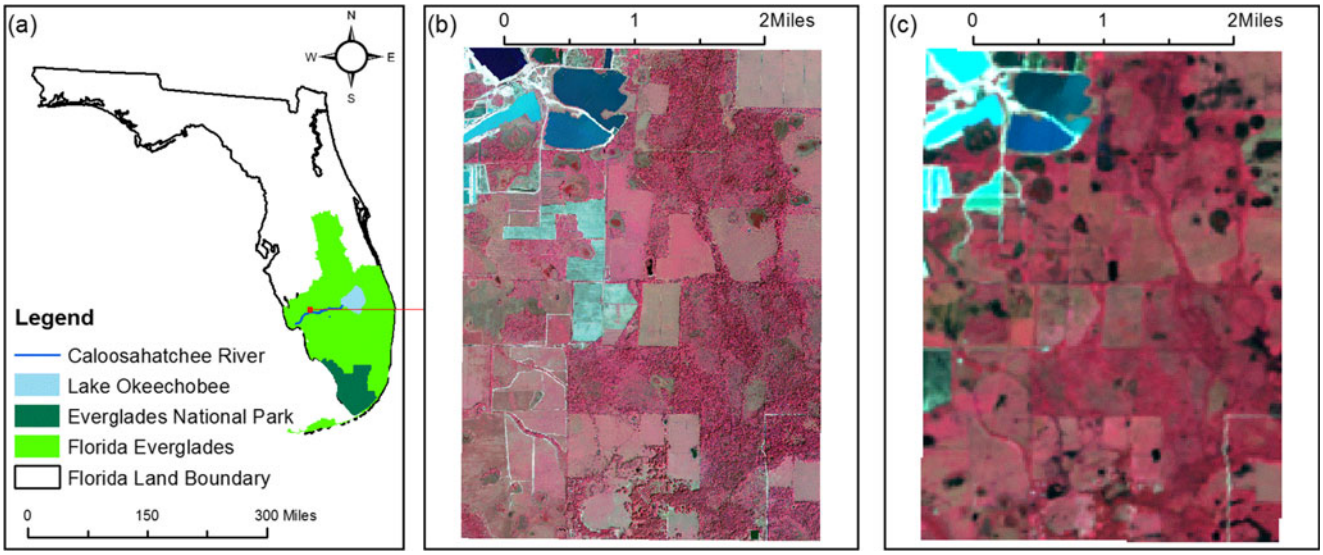

Fig. 1 Map of the Florida Everglades (**a**), and study site shown as a color infrared (CIR) 1-meter aerial photography (**b**), and a color composite from the 30-meter EO-1/Hyperion imagery (Bands 40, 30, and 20 as *red*, *green* and *blue*, respectively) (**c**)

were dropped, leaving 125 usable bands covering visible, near-infrared, and shortwave infrared for further analysis. After the noisy band elimination, an image-to-image registration was employed to georeference the hyperspectral data using the aerial photography. Hyperspectral data has a high dimensionality and contains a tremendous amount of redundant spectral information. The Minimum Noise Fraction (MNF) method (Green et al. 1988) is commonly used to reduce the high dimensionality and inherent noise of hyperspectral data. Previous studies have shown that MNF transformed data can significantly improve the accuracy of vegetation mapping in the Everglades (Zhang and Xie 2012). We thus conducted the MNF transformation for the hyperspectral imagery and selected the first nine MNF eigenimages which were the most useful and spatially coherent layers. For LiDAR data processing, the topographic effect was eliminated first by subtracting the Digital Terrain Model (DTM) value underneath each point from the elevation. This is known as data normalization in LiDAR remote sensing. Points with a normalized elevation less than 0.5 foot were considered as ground points and were not used in further analysis. Four DOQQ tiles were mosaicked and clipped for the study site.

Table 1 Vegetation communities and the number of reference image objects for each vegetation community in the study site

Vegetation types	Number of reference objects	Dominant species
1. Improved pastures	92	Dominated by a single grass species
2. Unimproved pastures	32	Dominated by a variety of native grasses
3. Woodland pastures	56	Dominated by a variety of native tree and shrub species
4. Field crops	110	Dominated by hay, grasses and sugar cane
5. Citrus groves	14	Oranges, grapefruits and tangerines
6. Upland shrub and brushland	28	Common species include gallberry, wax myrtle, saltbush, blueberries, rusty lyonia, fetterbush and other shrubs and brush, as well as various types of short herbs and grasses
7. Palmetto prairies	20	Dominated by Saw palmetto
8. Mixed rangeland	22	A mixture of herbaceous species and shrubs such as fetterbush, rusty Lyonia, dwarf blueberry and wax myrtle
9. Pine flatwoods	252	Dominant species include slash pine, saw palmetto, gall berry and various grasses
10. Mixed Wetland shrubs	18	A mixture of various shrubs
11. Freshwater marshes and wet prairies	94	Dominated by herbaceous vegetation

A Framework to Combine Three Remotely Sensed Data Sources

For this study a framework was designed to fuse three remotely sensed data to effectively map vegetation in the Everglades, as shown in Fig. 2. Data fusion methods can be grouped into three categories: pixel-, feature-, and decision-level fusion (Gómez-Chova et al. 2015). Pixel-level fusion combines raw data from multiple sources into single resolution data to improve the performance of image processing tasks. Information may be lost during the data resampling procedure if the spatial resolution of input data sources is different (Solberg 2006). Feature-level fusion extracts features (e.g., textures) from each individual data source and merges these features into one or more feature maps for further processing. Decision-level fusion conducts a preliminary classification for each individual data source first, and then combines the classification results into one outcome. Researchers most commonly adopt the pixel-level fusion method. For example, to combine LiDAR data with optical imagery, raster surfaces are generated first from LiDAR point clouds, and then combined with the optical imagery pixel by pixel. A major problem with using LiDAR in this way is the introduction of error in the raster surface generation step (Smith et al. 2004), which will ultimately affect the classification result. To overcome this problem, it is desirable to extract LiDAR elevation and intensity information from the original point cloud data.

Our designed framework combines all three data fusion methods in the mapping procedure. In the framework, the fine spatial resolution aerial photography is segmented first to generate image objects and extract object features (i.e., textures), which is detailed in next subsection. The extracted features are then combined with pixel-level values of hyperspectral data. This is achieved by first calculating a mean spectrum of hyperspectral pixels which are within an image object and then integrating the mean spectrum with the extracted aerial features of this object. For the LiDAR data, three types of information can be extracted: elevation, intensity, and topography. For each image object, LiDAR descriptive statistics (minimum, maximum, mean, and standard deviation) of elevation and intensity are calculated using all the non-ground vegetation points within an image object. Similarly, descriptive statistics of terrain elevation and slope for each image object are derived from the DTM using pixels within an object (Fig. 2). Recent studies (Zhang et al. 2013; Zhang 2014) have illustrated that

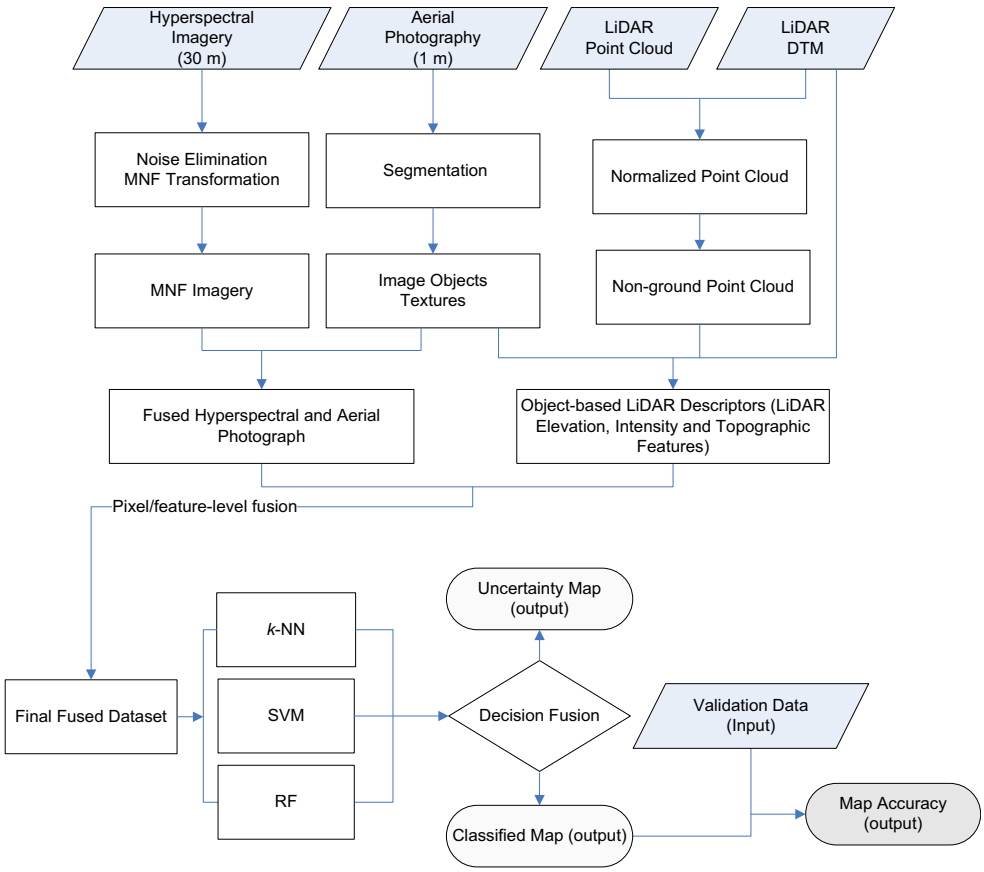

Fig. 2 The designed framework to combine three remotely sensed data sources for wetland vegetation mapping

extraction of LiDAR descriptors in this way is an effective approach for applying the low-posting-density LiDAR into the vegetation classification. All the LiDAR-derived features for each object are then joined with the pixel-level values of the hyperspectral imagery and feature-level of the aerial photograph, leading to a final fused dataset from three data sources. The fusion procedure combines pixel- and feature-level fusion methods at the object level, and thus this fusion scheme is referred to as the object-based pixel/feature-level fusion. Three machine learning classifiers (*k*-NN, SVM, and RF) are used to pre-classify the final fused dataset. The ultimate outcome is derived from ensemble analysis of three classification results using a decision-level fusion strategy. Note that our decision-level fusion strategy is based on classification results of the fused dataset, rather than making a decision from classification results of the individual data sources. The latter is commonly used in data fusion. Consequently, an object-based vegetation map is generated and evaluated by common accuracy assessment approaches. The ensemble analysis of three classification results also produces an uncertainty map which defines the confidence of the classification for each image object.

Five advantages are expected from the designed framework. First, no information is lost in the fusion strategy because there is no image resampling in the procedure. Common image fusion methods resample the fine spatial resolution (i.e., 1 meter) into medium-spatial resolution imagery (i.e., 30 meter) and then fuse two images pixel by pixel. This may lose valuable information in the fine spatial resolution imagery. Second, the local noise and heterogeneity can be effectively reduced. The remotely sensed signal for a pixel is affected by the surrounding pixels. Speckle frequently occurs due to intrinsic spectral variations. Using the averaged values all pixels within an object can reduce this effect, as well as the influence of marginal and unusually colored pixels (Dronova 2015). Third, additional object-based spatial information (i.e., texture) can be extracted from aerial photographs, which is useful in vegetation classification. Forth, small patches and linear/narrow shaped vegetation covers may be delineated due to the fine spatial resolution of aerial photograph. Application of 30-meter image alone is not able to delineate this type of features. Last, errors and uncertainties in the LiDAR data processing can be avoided because the original LiDAR point clouds are used instead of the LiDAR-generated raster layers. In addition, the object-based pixel/feature-level fusion scheme can also reduce the stripping effect caused by the calibration difference (Goodenough et al. 2003) in the EO-1/Hyperion sensor. The designed fusion scheme adopts the mean spectrum of the hyperspectral pixels within an object, which can help "smooth" the stripping over the segmented region, leading to a relatively homogeneous stripping effect across the entire scene. In this way the impact of stripping of EO-1/Hyperion in the classification can be reduced.

Image Segmentation and Feature Extraction of Aerial Photograph

Image segmentation is a major step in the designed framework. We used the multiresolution segmentation algorithm in eCognition Developer 9.0 (Trimble 2014) to generate image objects from the aerial photography. The segmentation algorithm starts with one-pixel image segments, and merges neighboring segments together until a heterogeneity threshold is reached. The heterogeneity threshold is determined by a user-defined scale parameter, as well as color/shape and smoothness/compactness weights. The scale parameter is an abstract term that determines the maximum allowed heterogeneity for the resulting objects. It decides the size of the objects with a small value generating more objects (small size), and a high value creating less objects (big size). The image segmentation is scale-dependent, and the quality of segmentation and classification depend on the scale of the segmentation. To find an optimal scale for image segmentation, an unsupervised image segmentation evaluation approach (Johnson and Xie 2011) was used. A scale of 60 was found to be optimal for the selected site and thus was used in this study. The minimum mapping unit is the smallest image object created from this scale parameter, which is 68 m^2 for the study site. Four spectral channels of the aerial photography were set to equal weights. Color/shape weights were set to 0.9/1.0 so that spectral information would be considered most heavily for segmentation. Smoothness/compactness weights were set to 0.5/0.5 so as to not favor either compact or non-compact segments. Following segmentation, object-based features of the aerial photograph were extracted. We extracted first-order and second-order metrics for each band of aerial photograph including mean, standard deviation, contrast, dissimilarity, homogeneity, entropy, and angular second moment. The grey level co-occurrence matrix (GLCM) algorithm was used to extract the second-order texture measures. Detailed algorithms can be found in Trimble (2014). These features from aerial photograph have proven valuable for vegetation mapping in the Everglades (Szantoi et al. 2013; Zhang et al. 2013; Zhang and Xie 2014; Szantoi et al. 2015) and thus were used for this study.

k-NN, SVM, and RF Classifiers

In the framework *k*-NN, SVM, and RF classifiers are employed to pre-classify the final fused dataset. *k*-NN is a supervised classifier which identifies objects based on the closest training samples in the feature space. It searches away from the unknown object to be classified in all directions until it encounters *k* user-specified training objects. It then assigns the object to the class with the majority vote of the encountered objects. SVM is a non-parametric supervised machine learning classifier. The aim of SVM is to find a hyperplane

that can separate the input dataset into a discrete predefined number of classes in a fashion consistent with the training samples (Vapnik 1995). SVM research in remote sensing has increased in the past decade, as reviewed by Mountrakis et al. (2010). Detailed descriptions of SVM algorithms were given by Huang et al. (2002) in the context of remote sensing. Kernel based SVMs are commonly used in classification, among which the radial basis function (RBF) and the polynomial kernels are frequently employed. RBF needs to set the kernel width (γ), and the polynomial kernel needs to set the degree (p). Both kernels need to define a penalty parameter (C) that controls the degree of acceptable misclassification (Hsu et al. 2010). Both kernels were tested in this study to find the best model for the final fused dataset. RF is a decision tree based ensemble classifier which is valuable in processing hyperspectral imagery. Detailed descriptions of RF can be found in Breiman (2001) and in a remote sensing context by Chan and Paelinckx (2008). Two parameters need to be defined in RF: the number of decision trees to create (k) and the number of randomly selected variables (M) considered for splitting each node in a tree. RF is not sensitive to M and it is often blindly set to $\sqrt{M}$ (Gislason et al. 2006). k is often set based on trial and error.

Ensemble Analysis

In the framework ensemble analysis is employed to generate the final vegetation map from the outputs of k-NN, SVM, and RF. An ensemble analysis approach is a multiple classification system that combines the outputs of several classifiers. The classifiers in the system should generally produce accurate results but show some differences in classification accuracy (Du et al. 2012). A range of strategies were developed to combine the outputs from multiple classifiers. Among them the majority vote (each individual classifier votes for an unknown input object) is straightforward. A key problem of the majority vote is that all the classifiers have equal rights to vote without considering their performances on each individual class. A weighting strategy may mitigate this problem by weighting the decision from each classifier based on their accuracies obtained from the reference data (Moreno-Seco et al. 2006). For this study the majority vote and the weighting strategy were combined to analyze the outputs from three classifiers. If three votes are different for an unknown object (e.g., k-NN votes class 1, SVM votes class 2, and RF votes class 3), then the unknown object will be assigned to the class which has the highest accuracy among the classifiers (e.g., class 3 because RF has the highest accuracy among k-NN, SVM, and RF in identifying class 1, class 2, and class 3 respectively). That is, the classifier with the best performance among three votes will obtain a weight of 1, while weights of the other two classifiers will be set at 0. If two or three classifiers vote the same class for an input object, then the object will be assigned to the same voted class. An uncertainty map can also be derived from the ensemble analysis of three classifiers. If three classifiers vote the same class for an unknown image object, a complete agreement will be achieved. Conversely if three votes are completely different, no agreement will be obtained. If only two classifiers vote for the same class, a partial agreement will be produced. Consequently the uncertainty map will be produced in conjunction with the final classified map from the ensemble analysis.

Accuracy Assessment

The error matrix and Kappa statistic (Congalton and Green 2009) has served as the standard approach in accuracy assessment. An error matrix was constructed for the final classified map and the Kappa statistics were calculated. To evaluate the statistical significance of differences in accuracy between different classifications, the nonparametric McNemar test (Foody 2004) was adopted. The difference in accuracy for a pair of classifications is considered as being statistically significant at a confidence of 95 % if z-score is larger than 1.96 in the McNemar test.

Results

Experimental Analysis

A total of 12 experiments (see Table 2) were designed to evaluate the framework using different classifiers and datasets. Experiments 1–3 applied the aerial photograph alone; Experiments 4–6 fused the aerial photograph and hyperspectral imagery; Experiments 7–9 combined the aerial photograph and LiDAR data; and Experiments 10–12 integrated the three data sources. A number of tests were also conducted to reveal the optimal specification of the parameters required by each classifier. Application of the aerial photography alone produced a result using the three classifiers with overall accuracies varying from 69.6 to 72.9 % and Kappa values ranging from 0.63 to 0.67 (Experiments 1–3). The RF classifier generated the best result in these three experiments. A combination of the aerial photography and EO-1/Hyperion imagery consistently increased the classification with a varying overall accuracy (82.7–84.6 %) and Kappa value (0.79–0.81) (Experiments 4–6). An integration of the aerial photography with LiDAR also improved the classification compared with using the aerial photography alone, which produced a range of 82.7–85.1 % in overall accuracies and 0.79–0.81 in Kappa values (Experiments 7–9). McNemar tests between the classifications of the aerial photography alone and a fusion of the two data sources showed that the improvements of two data sources were statistically

Table 2 Classification accuracies and statistical tests from different datasets and classifiers

Aerial photography				
Experiment	Overall accuracy (%)	Kappa value	z-Score (Kappa)	z-Score (McNemar)
1. *k*-NN	71.3	0.65	23.9	4.91*; 4.64 (1/4; 1/7)
2. SVM	69.6	0.63	22.2	6.44*; 6.04 (2/5; 2/8)
3. RF	72.9	0.67	24.5	4.81*; 4.65 (3/6; 3/9)
Aerial photography and hyperspectral imagery				
4. *k*-NN	83.2	0.80	35.1	4.42* (4/13)
5. SVM	84.6	0.81	36.3	3.62* (5/13)
6. RF	82.7	0.79	33.4	4.62* (6/13)
Aerial photography and LiDAR				
7. *k*-NN	82.7	0.79	33.5	4.73* (7/13)
8. SVM	85.1	0.82	37.2	3.89* (8/13)
9. RF	82.7	0.79	33.5	4.73* (9/13)
Aerial photography, hyperspectral imagery, and LiDAR				
10. *k*-NN	88.1	0.86	42.9	2.52* (10/13)
11. SVM	90.5	0.88	48.6	0.63 (11/13)
12. RF	87.5	0.85	41.5	2.71* (12/13)
13. EA	91.1	0.89	48.9	NA

k-NN *k*-Nearest Neighbor; *SVM* Support Vector Machine; *RF* Random Forest; *EA* Ensemble Analysis of *k*-NN, SVM, and RF; *: significant with 95 % confidence; For the McNemar tests 1/4, 1/7, 2/5,…12/13 refer to the test between Experiments 1 and 4, 1 and 7, 2 and 5,… 12 and 13, respectively

significant. The best result was achieved by fusing three data sources which produced the overall accuracies ranging from 87.5 to 90.5 % and Kappa values from 0.85 to 0.88 (Experiments 10–12). The SVM produced the highest overall accuracy (Experiment 11) when three data sources were combined. Kappa z-score statistical tests revealed that all the classifications from Experiments 1–12 were significantly better than a random classification.

Ensemble Analysis

The designed Experiments 1–12 demonstrated that a synergy of the three data sources was the best solution in mapping vegetation types. Three classifiers generated a comparable result. The per-class accuracies from Experiments 10–12 are listed in Table 3. Performances of the three classifiers were not complete even in identifying each class. For example from the user's perspective, *k*-NN produced the best result in characterizing classes 2, 3 and 11; SVM had the best performance in discriminating classes 1, 4, 5, 7 and 9; and RF showed the highest accuracy in classifying classes 8, and 10. From the producer's perspective, *k*-NN was the best in discriminating classes 4 and 5; SVM was the best in identifying 1, 8, and 9; and RF produced the highest accuracy for classes 2, and 7. This diversity is primarily caused by the discrepancies in concepts of the three algorithms. *k*-NN searches for the best match to denote inputs; RF looks for optimal decision trees to group data, whereas SVM explores for the optimal hyperplane to categorize data. The diversity of the three classifications drives the exploration of the ensemble analysis. The difference in outputs from multiple classifiers is an assumption of classifier ensemble techniques. The ensemble analysis result is displayed as Experiment 13 in Table 2. It increased the classification with a total accuracy of 91.1 % and a Kappa value of 0.89.

McNemar tests were conducted between the classification of ensemble analysis (Experiment 13) and classifications from Experiments 4–12. The z-score values in McNemar tests showed that the improvement from a synergy of three data sources was statistically significant compared with the fusion of two data sources. The improvement from ensemble analysis was also statistically significant compared with the *k*-NN and RF classifiers. However, there was no significant difference in classification between ensemble analysis and SVM (see Table 2).

Object-Based Vegetation Map and Uncertainty Map from Ensemble Analysis

Landis and Koch (1977) suggested that Kappa values larger than 0.80 indicate strong agreement or accuracy. The designed framework produced a Kappa value of 0.89 (Experiment 13), showing the designed framework is effective for vegetation mapping. An object-based vegetation map was thus produced using the fused dataset of the three data sources and ensemble analysis of three

Table 3 Per-class accuracies derived from the fused dataset of three data sources using three classifiers; the highest accuracy among three classifiers is highlighted in bold

Classes	User's accuracy (%)			Producer's accuracy (%)		
	k-NN	SVM	RF	*k*-NN	SVM	RF
1. Improved pastures	87.5	**95.6**	90.7	95.5	**97.7**	88.6
2. Unimproved pastures	**86.7**	84.6	82.4	81.3	68.8	**87.5**
3. Woodland pastures	**65.4**	63.0	57.1	100.0	100.0	94.1
4. Field crops	96.4	**98.1**	94.4	**91.5**	89.8	86.4
5. Citrus groves	88.9	**100.0**	87.5	**88.9**	77.8	77.8
6. Upland shrub and brushland	92.9	92.9	85.7	92.9	92.9	85.7
7. Palmetto prairies	76.9	**100.0**	73.3	66.7	66.7	**73.3**
8. Mixed rangeland	50.0	83.3	**100.0**	90.0	**100.0**	40.0
9. Pine flatwoods	96.7	**97.5**	95.2	95.9	**97.5**	97.5
10. Mixed Wetland Shrubs	66.7	80.0	**87.5**	35.3	47.1	41.2
11. Freshwater marshes and wet prairies	**90.0**	78.2	81.1	78.3	93.5	93.5

classifiers, as shown in Fig. 3(a). The study area was dominated by pine flatwoods, crops, and pastures which were relatively homogeneous and well characterized. Small patches and linear/narrow shaped features were also successfully mapped such as marshes and wetland shrubs. The object-based vegetation map is more informative and useful than a traditional pixel-based one that may be noisy if the study area has a high degree of spatial and spectral heterogeneity. An error matrix was also constructed for the classified map, as shown in Table 4. The user's accuracies ranged from 60.7 % (class 3) to 100 % (classes 5 and 7). The producer's accuracies varied from 41.2 % (class 10) to 100 % (class 3).

The corresponding uncertainty map is shown as Fig. 3(b). A major portion had a complete agreement from three classifiers (shown in green), indicating the highest confidence being correctly classified. Some areas (shown in blue) were voted by two classifiers, generating a partial agreement in classification. A few regions displayed a "warning sign" (shown in red), where no classification agreement was obtained. These regions had the highest probability of being misclassified. The uncertainty map demonstrated the classified map was robust. The traditional accuracy assessment approaches such as the overall accuracy, and producer's and user's accuracies only present the quantitative evaluation. No spatial information can be provided by such approaches. The ensemble analysis is able to effectively identify regions easy to classify and areas challenging to discriminate by developing this type of uncertainty map with geographic locations provided. This type of map is useful when there is a desire to minimize the omission or commission errors. It also can be used to guide the post-classification fieldwork (Foody et al. 2007). Studies of this type of map are very limited. Further research is needed to investigate the potential application of such maps in remote sensing.

Discussion

Benefits of Data Fusion for Vegetation Mapping

Several efforts have been made for automating vegetation mapping in the Everglades using data fusion techniques given the fact that the application of most available remote sensing data alone cannot produce requisite results for CERP. The first effort is from Griffin et al. (2011) who integrated Landsat imagery, soil data, and a digital elevation model for mapping the Kissimmee prairie watershed in the northern Everglades. The second effort is from Szantoi et al. (2013) who combined aerial photography, soil depth layer, and four hydrological variables to map wet graminoid/sedge communities in a portion of the Everglades National Park. Zhang et al. (2013) integrated aerial photography and LiDAR to map forest community. Most recently, a combination of hyperspectral imagery and LiDAR (Zhang 2014) and a synergy of aerial photography and hyperspectral imagery (Zhang and Xie 2014) were evaluated to map vegetation communities in the Everglades. They assessed what detail level and accuracy could be produced and the contribution of three LiDAR features (elevation, intensity, and topography) in the classification. The results illustrated that a combination of two data sources produced a higher accuracy than the application of single data source, and the three LiDAR features had the same contribution in the classification.

To enhance the application of data fusion techniques in the Everglades, in this study we assessed the potential of fusing three data sources carrying complimentary information for vegetation mapping. Aerial photography has a fine spatial resolution but limited spectral resolution. The EO-1/Hyperion hyperspectral imagery has a fine spectral resolution but coarse spatial resolution. Hyperspectral imaging relies primarily on spectral features to discriminate covers, whereas

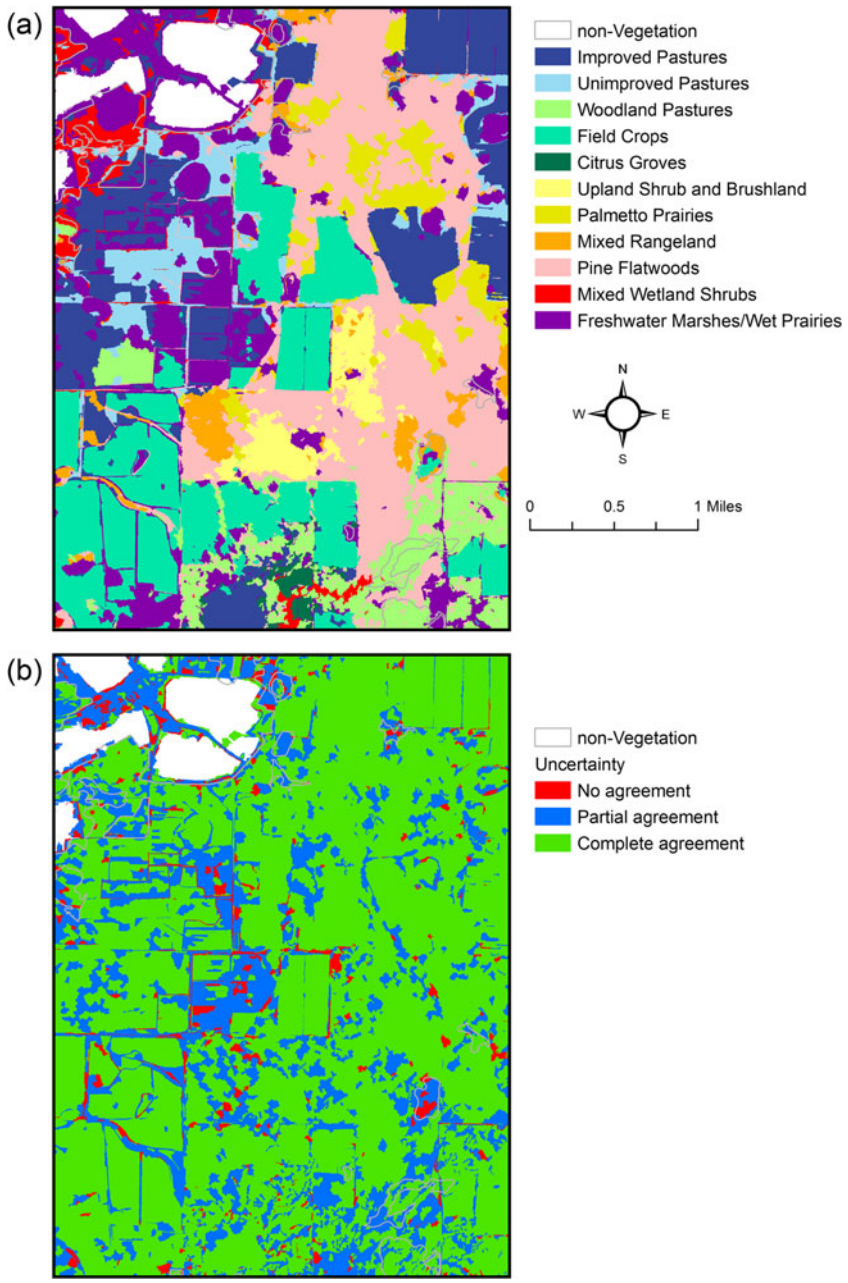

Fig. 3 (**a**) Classified vegetation map from the fused dataset and ensemble analysis of the outputs of three classifiers; and (**b**) the uncertainty map generated from ensemble analysis of three classifiers

fine spatial resolution aerial photography relies more on spatially invariant features to identify targets (Shaw and Burke 2003). A combination of these two types of optical imagery may improve the classification. Fusing 1-meter aerial photography and 30-m hyperspectral imagery does indeed improve the classification. This confirms the conclusion in Zhang and Xie (2014) who mapped nine vegetation species in the coastal Everglades by fusing aerial photography and 20-m airborne hyperspectral imagery.

Previous studies have proven the gain from low-posting-density LiDAR for Everglades mapping, which drives the inclusion of LiDAR in the framework. An integration of LiDAR with aerial photography and hyperspectral imagery achieved the best result, indicating the effectiveness of the designed framework. The developed object-based pixel/feature-level fusion scheme successfully combines the spatial features of aerial photography, rich spectral contents of hyperspectral imagery, and elevation, intensity, and low-posting-density LiDAR features. It complements the shortages and takes advantage of the benefit of each individual data source. Application of data fusion is critical for the achieved result.

Note that there were time gaps in the acquisition of aerial photography (November 2004), EO-1/Hyperion hyperspectral imagery (October 2005), and LiDAR data (December 2007). Topographic features might not have changed too much in

Table 4 Error matrix of the final classified map

Class #	1	2	3	4	5	6	7	8	9	10	11	Row Total	PA (%)
1	43			1								44	97.7
2		13								1	2	16	81.4
3			17									17	100.0
4	2			54							3	59	91.5
5			2		7							9	77.8
6						13			1			14	92.9
7	1					1	10	1	2			15	66.7
8								9	1			10	90.0
9								1	121			122	99.2
10		3	7							7		17	41.2
11			2						1	1	42	46	91.3
Col. Total	46	16	28	55	7	14	10	11	126	9	47	Overall accuracy: 91.1 %	
UA (%)	93.5	81.3	60.7	98.2	100.0	92.9	100.0	81.8	96.0	77.8	89.4	Kappa value: 0.89	

PA Producer's Accuracy; *UA* User's Accuracy; Classification result is displayed in row, and the reference data is displayed in column; The name of each class is displayed in Table 1

3 years, but vegetation structure characterized by LiDAR might have been severely changed. Simultaneous collection of three data sources may be able to produce a better result.

Advantages of Machine Learning Classifiers and Ensemble Analysis

Previous studies have illustrated that the three classifiers *k*-NN, SVM, and RF are powerful in classifying hyperspectral imagery and fused datasets. Here we evaluated their performance for processing a single-source dataset, two-source dataset, and three-source dataset. Three classifiers obtained a comparable result but showed diversity in per-class accuracy. This drives the application of ensemble analysis technique in the framework. Ensemble analysis indeed increased the classification accuracy and the improvement was statistically significant. In addition, the ensemble analysis provided an uncertainty map which presented complementary information to the error matrix of the classified map. It identified the geographic regions with a high robust classification and areas where classification errors were most likely to occur. This type of uncertainty analysis has a great potential in remote sensing. Ensemble analysis makes the classification more robust.

Summary and Conclusions

For this study we designed a framework to combine three complimentary remotely sensed datasets for automated vegetation mapping in the Everglades. To effectively determine the benefits of each individual data source, an object-based pixel/feature-level fusion scheme was developed, and a decision-level fusion strategy was applied by ensemble analysis of three machine learning classifiers. Testing of the framework in a portion of the central Everglades achieved an overall accuracy of 91.1 % and a Kappa value of 0.89 for mapping eleven vegetation types. We draw the following conclusions from this study:

1) Hyperspectral and LiDAR systems are valuable for delineating wetland vegetation land covers. Combining hyperspectral imagery with aerial photography or LiDAR with aerial photography through fusing two data sources significantly improves the classification accuracy compared with applying the aerial photography alone.
2) A fusion of three data sources shows the promise to map diverse vegetation communities in complex wetlands. An integration of three data sources significantly improves the classification compared with the application of two data sources.
3) Three machine learning classifiers (*k*-NN, SVM, and RF) are useful in processing the fused dataset from multiple sources. All of them performed well in the classification. Ensemble analysis is beneficial in the framework. It not only increased the classification, but it also provided an important uncertainty map which complemented the traditional accuracy assessment approaches.
4) The designed framework can be used as an alternative to the current manual procedure for updating and building vegetation databases in the Everglades. CERP largely collects aerial photographs; the EO-1/Hyperion is still on orbit and acquiring hyperspectral imagery; low-posting-density LiDAR is available for many regions in the Everglades. Fusing three data sources has a potential to

map broad areas in the Everglades with a reduced cost. With the increasing availability of three types of data it is anticipated this study can benefit the global wetland mapping in general, and the Florida Everglades in particular.

References

Adam E, Mutanga O, Rugege D (2010) Multispectral and hyperspectral remote sensing for identification and mapping of wetland vegetation: a review. Wetl Ecol Manag 18:281–296

Blaschke T (2010) Object based image analysis for remote sensing. ISPRS J Photogramm Remote Sens 65:2–16

Breiman L (2001) Random forests. Mach Learn 45:5–32

Chan JC-W, Paelinckx D (2008) Evaluation of random forest and adaboost tree based ensemble classification and spectral band selection for ecotope mapping using airborne hyperspectral imagery. Remote Sens Environ 112:2999–3011

Comprehensive Everglades Restoration Plan (CERP), http://www.evergladesplan.org/ (last data accessed: 25 September 2015)

Congalton R, Green K (2009) Assessing the accuracy of remotely sensed data: principles and practices, 2nd edn. CRC/Taylor & Francis, Boca Raton

Doren RF, Rutchey K, Welch R (1999) The Everglades: a perspective on the requirements and applications for vegetation map and database products. Photogramm Eng Remote Sens 65:155–161

Dronova I (2015) Object-based image analysis in wetland research: a review. Remote Sens 7:6380–6413

Du P, Xia J, Zhang W, Tan K, Liu Y, Liu S (2012) Multiple classifier system for remote sensing image classification: a review. Sensors 12:4764–4792

Folkman M, Pearlman J, Liao L, Jarecke P (2001) EO1/Hyperion hyperspectral imager design, development, characterization and prediction, in: Smith WL, Yasuoka Y (Eds.), Hyperspectral Remote Sensing of the Land and Atmosphere, SPIE Proc, 4151: 40–51

Foody GM (2004) Thematic map comparison, evaluating the statistical significance of differences in classification accuracy. Photogramm Eng Remote Sens 70:627–633

Foody GM, Boyd DS, Sanchez-Hernandez C (2007) Mapping a specific class with anensemble of classifiers. International Journal of Remote Sensing 28:1733–1746

Gislason PO, Benediktsson JA, Sveinsson JR (2006) Random forests for land cover classification. Pattern Recogn Lett 27:294–300

Gómez-Chova L, Tuia D, Moser G, Camps-Valls G (2015) Multimodal classification of remote sensing images: a review and future directions. Proc IEEE 103:1560–1584

Goodenough DG, Dyk A, Niemann KO, Pearlman JS, Chen H, Han T, Murdoch M, West C (2003) Processing hyperion and ALI for forest classification. IEEE Trans Geosci Remote Sens 41:1321–1331

Green AA, Berman M, Switzer P, Craig MD (1988) A transformation for ordering multispectral data in terms of image quality with implications for noise removal. IEEE Trans Geosci Remote Sens 26:65–74

Griffin S, Rogan J, Runfola DM (2011) Application of spectral and environmental variables to map the Kissimmee prairie ecosystem using classification trees. GIScience Remote Sensing 48:299–323

Hirano A, Madden M, Welch R (2003) Hyperspectral image data for mapping wetland vegetation. Wetlands 23:436–448

Hsu C, Chang C, Lin C (2010) A practical guide to support vector classification. Final report, National Taiwan University, Taipei City

Huang C, Davis LS, Townshend JRG (2002). An assessment of support vector machines for land cover classification. International Journal of Remote Sensing 23:725–749

Jensen J, Rutchey K, Koch M, Narumalani S (1995) Inland wetland change detection in the Everglades water conservation area 2A using a time series of normalized remotely sensed data. J Photogrammetric Eng Remote Sensing 61:199–209

Johnson B, Xie Z (2011) Unsupervised image segmentation evaluation and refinement using a multi-scale approach. ISPRS J Photogramm Remote Sens 66:473–483

Jones JW (2011) Remote sensing of vegetation pattern and condition to monitor changes in Everglades biogeochemistry. Crit Rev Environ Sci Technol 41:64–91

Ke Y, Quackenbush LJ, Im J (2010) Synergistic use of QuickBird multispectral imagery and LiDAR data for object-based forest species classification. Remote Sens Environ 114:1141–1154

Kloiber SM, Macleod RD, Smith AJ, Knight JF, Huberty BJ (2015) A semi-automated, multi-source data fusion update of a wetland inventory for east-central Minnesota, USA. Wetlands. doi:10.1007/s13157-014-0621-3

Landis J, Koch GG (1977). The measurement of observer agreement for categorical data. Biometics 33:159–174

Lewis P, Hancock S (2007) LiDAR for vegetation applications. In UCL Gower St, London

McPherson BF, Halley R (1996) The south Florida environment—A region under stress, U.S. Geological Survey Circular 1134

Moreno-Seco F, Iñesta J, de León P, Micó L (2006) Comparison of classifier fusion methods for classification in pattern recognition tasks. Proceedings of the joint IAPR international conference on Structural, Syntactic, and Statistical Pattern Recognition, pp. 705–713

Mountrakis G, Im J, Ogole C (2010) Support vector machines in remote sensing: a review. ISPRS J Photogramm Remote Sens 66:247–259

Onojeghuo AO, Blackburn GA (2011) Optimising the use of hyperspectral and LiDAR data for mapping reedbed habitats. Remote Sens Environ 115:2025–2034

Rutchey K, Vilchek L (1994) Development of an Everglades vegetation map using a SPOT image and the global positioning system. Photogramm Eng Remote Sens 60:767–775

Rutchey K, Vilchek L (1999) Air photointerpretation and satellite imagery analysis techniques for mapping cattail coverage in a northern Everglades impoundment. Photogramm Eng Remote Sens 65:185–191

Rutchey K, Schall T, Sklar F (2008) Development of vegetation maps for assessing Everglades restoration progress. Wetlands 28:806–816

Shaw GA, Burke HK (2003) Spectral imaging for remote sensing. Lincoln Laboratory J 14:3–28

Smith SL, Holland DA, Longley PA (2004) The importance of understanding error in LiDAR elevation models. Proceedings of the ISPRS Congress, Istanbul, pp 12–23

Solberg AHS (2006) Data fusion for remote sensing applications. In: Chen CH (ed) Signal and image processing for remote sensing. CRC Press, Boca Raton, pp 515–537

Szantoi Z, Escobedo F, Abd-Elrahman A, Smith S, Pearlstine L (2013) Analyzing fine-scale wetland composition using high resolution imagery and texture features. Int J Appl Earth Observation Geoinformation 23:204–212

Szantoi Z, Escobedo F, Abd-Elrahman A, Pearlstine L, Dewitt B, Smith S (2015) Classifying spatially heterogeneous wetland communities using machine learning algorithms and spectral and textural features. Environ Monitoring Assessment, 187

Thenkabail PS, Lyon GJ, Huete A (2011) Hyperspectral remote sensing of vegetation. CRC Press, Boca Raton

Trimble (2014) eCognition developer 9.0.1 reference book

Vapnik VN (1995) The nature of statistical learning theory. Springer-Verlag, New York

Waske B, Benediktsson JA, Árnason K, Sveinsson JR (2009) Mapping of hyperspectral AVIRIS data using machine-learning algorithms. Can J Remote Sens 35:S106–S116

Zhang C (2014) Combining hyperspectral and LiDAR data for vegetation mapping in the Florida Everglades. Photogramm Eng Remote Sens 80:733–743

Zhang C (2015) Applying data fusion techniques for benthic habitat mapping and monitoring in a coral reef ecosystem. ISPRS J Photogramm Remote Sens 104:213–223

Zhang C, Qiu F (2012) Mapping individual tree species in an urban forest using airborne LiDAR data and hyperspectral imagery. Photogramm Eng Remote Sens 78:1079–1087

Zhang C, Xie Z (2012) Combining object-based texture measures with a neural network for vegetation mapping in the Everglades from hyperspectral imagery. Remote Sens Environ 124:310–320

Zhang C, Xie Z (2013) Object-based vegetation mapping in the Kissimmee river watershed using HyMap data and machine learning techniques. Wetlands 33:233–244

Zhang C, Xie Z (2014) Data fusion and classifier ensemble techniques for vegetation mapping in the coastal Everglades. Geocarto Int 29:228–243

Zhang C, Xie Z, Selch D (2013) Fusing LiDAR and digital aerial photography for object-based forest mapping in the Florida Everglades. GIScience Remote Sensing 50:562–573